

# Mars Exploration Rover Parachute System Performance

Allen Witkowski\* and Dr. Mike Kandis†  
*Pioneer Aerospace, S. Windsor, CT, 06074*

Dr. Robin Bruno‡  
*Jet Propulsion Laboratory, Pasadena, CA, 91105*

and

Dr. Juan Cruz§  
*NASA Langley Research Center, Hampton, VA, 23681*

The Mars Exploration Rover (MER) program successfully landed two rovers, named “Spirit” and “Opportunity”, on the surface of Mars in January 2004. Critical to the Entry, Descent, and Landing (EDL) process, was the performance of the Parachute Decelerator System (PDS) that consisted of a mortar deployed, 14.1 meter diameter Disk Gap Band (DGB) parachute. Prior to the first EDL, analyses were conducted to predict “nominal” parachute performance, based on navigation estimates of initial conditions and using models generated during the development program. Uncertainty in atmospheric properties, due in part to a dust storm in the month prior to landing, required review of the timing, and hence dynamic pressure, at which to initiate mortar deployment. This paper details critical system design features, as related to the performance postulated from returned data, and describes current best estimates for deployment system performance, parachute drag coefficient, inflation performance, inflation loads, and terminal descent. Despite the uncertainties involved, the pre-landing predictions matched well with the returned flight performance data.

## Nomenclature

$C_D$	=	parachute drag coefficient
$\sigma$	=	standard deviation
MER	=	Mars Exploration Rover
EDL	=	Entry Descent and Landing
PDS	=	Parachute Decelerator System
DGB	=	Disk Gap Band
MDS	=	Mortar Deployment Subsystem
RAD	=	Rocket Assisted Deceleration
$F_p$	=	Force generated by the parachute during inflation
$g$	=	Acceleration due to gravity
$k_0$	=	Non-dimensional apparent mass coefficient
$m_a$	=	Parachute apparent mass
$m_p$	=	Parachute mass
$q$	=	Dynamic pressure
$S_p$	=	Projected parachute area
$S_{p_{max}}$	=	Maximum projected parachute area

---

\* Principal Engineer Space & Special Projects, Member AIAA.

† Analytical Engineer, Member AIAA.

‡ Contract Technical Manager, Mechanical Systems, Mail Stop 157-500.

§ Insert Job Title, Exploration Systems Engineering Branch, Mail Stop 489, Member AIAA.

$S_r$	= Parachute projected area ratio
$S_0$	= Nominal parachute area
$t$	= Time
$t_{inf}$	= Parachute inflation time
$t_r$	= Parachute inflation time ratio, $t/t_{inf}$
$V$	= Velocity or airspeed
$\Gamma_0$	= Volume of a hemisphere with diameter equal to $D_0$
$\rho$	= Fluid density
$\gamma$	= Flight path angle measured from horizontal

## I. Introduction

THE Mars Exploration Rover Program landed two rovers on the surface of Mars in January of 2004 to look for evidence of past water. The MER A “Spirit” landed in Gusev Crater on January 4, 2004 and MER B “Opportunity” landed in Eagle Crater on Meridiani Planum on January 25, 2004. The rovers utilized nearly the same EDL architecture developed for the 1996-97 Mars Pathfinder mission. Yet unlike the Mars Pathfinder rover/lander system, these rovers accommodate the entire science package, including avionics, sensors, and communication equipment, with the lander shell discarded following landing. Each rover is a mobile platform with numerous scientific sensors designed to provide geologic data including mineral composition, Iron content, and imaging. Both rovers continued operation well beyond their design requirements for 90 sols duration and 600 meters distance traveled. More significantly, both rovers discovered geologic evidence for past water, strengthening the argument for further exploration in the search for past or present life. These accomplishments would not have been possible without a successful landing in which EDL architecture played a key role. The EDL architecture utilized a DGB parachute that was deployed following atmospheric entry and peak deceleration/peak heating. This parachute served the purpose of further decelerating the spacecraft, altering the flight path vector from nearly horizontal to nearly vertical with respect to the planet’s surface, and provided a stable platform for the remaining descent and landing tasks (heatshield release, radar ground acquisition, airbag inflation, descent imaging, etc.). The Parachute Decelerator System (PDS) consists of a mortar deployed 14.1 meter diameter, DGB parachute with band length equal to 1.8 times an equivalent Viking DGB. The PDS developed for MER is described in reference 1 while the Mortar Deployment Subsystem (MDS) is described in reference 2.

The thin Martian atmosphere makes validation/verification testing of the PDS difficult to conduct on Earth. Realistic full-scale testing would involve accelerating a test vehicle to supersonic speeds at altitudes near 36 km. Such demanding requirements led to little to no testing or data collection on the full-scale performance of these canopy types since 1972. Therefore, each landing is, in effect, an additional flight test of this canopy design and an opportunity to add to the full-scale database. This mission also allowed for the unique opportunity to alter the operation of the second EDL, based on analysis of collected data from the first EDL, and was warranted due to changes in atmospheric density caused by a dust storm post-launch/pre-landing. This report documents the current performance models for this PDS design and presents the state of predictive ability based on those models.

## II. Performance Estimating Prior To Landing

The numerical model used to predict parachute performance during inflation is based upon a variant of equations utilized by numerous authors<sup>3,4</sup>. Parachute inflation is modeled as beginning at bag strip, which is defined as the moment the deployment bag separates from the apex of the parachute. From this point to full inflation, the force generated by the parachute is modeled as:

$$F_p = qC_D S + \frac{d}{dt} \{ (m_a + m_p) V \} - m_p g \cdot \sin \gamma \quad (1)$$

where  $q$  is the dynamic pressure,  $C_D S$  is the parachute drag area,  $m_a$  is the apparent mass (of the fluid),  $m_p$  is the mass of the parachute,  $V$  is the velocity or airspeed,  $g$  is the acceleration of gravity, and  $\gamma$  is the flight path angle. Performing the indicated differentiation yields:

$$F_p = qC_D S + (m_a + m_p) \frac{dV}{dt} + \frac{dm_a}{dt} V - m_p g \bullet \text{Sin} \gamma \quad (2)$$

The apparent fluid mass is described by:

$$m_a = k_0 \rho \Gamma_0 S_r^{3/2} \quad (3)$$

where  $\rho$  is the fluid density and  $\Gamma_0$  is the volume of a hemisphere with a diameter equal to the nominal diameter of the parachute,  $D_0$ :  $\Gamma_0 = \pi D_0^3 / 12$ .  $S_r$  is the non-dimensional parachute projected area ratio,  $S_r = S_p / S_{p_{\max}}$ , where  $S_p$  is the projected parachute area at any given time during the inflation and  $S_{p_{\max}}$  is the maximum projected parachute area. The non-dimensional coefficient  $k_0$  is constant and empirically derived from test data as discussed later in this section. Differentiation of equation 3 results in:

$$\frac{dm_a}{dt} = k_0 \frac{d\rho}{dt} \Gamma_0 S_r^{3/2} + \frac{3}{2} k_0 \rho \Gamma_0 S_r^{1/2} \frac{dS_r}{dt} \quad (4)$$

The term  $C_D S$  is approximated as:

$$C_D S = C_{D_0} S_0 S_r \quad (5)$$

where  $C_{D_0}$  is the steady-state parachute drag coefficient for the fully inflated parachute and  $S_0$  is the nominal parachute area. Substituting equations 3, 4, and 5 into equation 2, and neglecting smaller order terms (i.e.,  $m_p$  and  $d\rho/dt$ ), yields the basic equation for prediction of opening loads:

$$F_p = qC_{D_0} S_0 S_r + k_0 \rho \Gamma_0 S_r^{3/2} \frac{dV}{dt} + \frac{3}{2} k_0 \rho \Gamma_0 S_r^{1/2} \frac{dS_r}{dt} V \quad (6)$$

Solving this equation for the peak opening load requires several experimentally determined parameters as inputs. Primary among these are the inflation profile ( $S_p$  as a function of inflation time) and the apparent mass coefficient ( $k_0$ ). Video recordings of the inflation process during low altitude drop tests and wind tunnel testing were used to reconstruct the projected canopy area ratio ( $S_r$ ) as a function of inflation time ratio ( $t_r$ ). This method provides a simple means for comparing and averaging projected area data for tests having disparate inflation times. Next, the measured peak opening load and remaining known values can be substituted into equation 6, at the time of peak opening load, to determine an appropriate apparent mass coefficient. This process was applied to the numerous tests performed during this program to the development a best-fit inflation profile and value for  $k_0$ . Yet all of the test data regarding inflation was obtained from low speed, high atmospheric density tests conducted on Earth. Studies have shown potentially significant differences in the inflation time of parachutes tested from low to high altitudes<sup>5</sup> where the atmospheric density may decrease by orders of magnitude (as they would on Mars). In light of this fact, test data from programs involving high altitude, low atmospheric density deployments of DGB parachutes (i.e., Viking BLDT, Mars Pathfinder, PEPP, and SPED) were used to develop an empirically-based model for calculating inflation time under conditions comparable to those expected during a Mars EDL. This empirical model adjusted the value of  $t_{inf}$  but the relationship of  $S_r$  to  $t_r$  was held constant.

The numerical model was discussed above was used to provide predictions for the time to peak load and peak opening load prior to the first EDL. Obviously, the precise initial conditions at mortar firing were not known at the time so several test cases were examined. These test cases utilized initial values for the Mach number and dynamic pressure that spanned the expected flight envelope at mortar firing. Following each landing, additional simulations were performed using the nominal reconstructed values for Mach number and dynamic pressure as inputs. The predicted peak opening loads from these efforts are listed in Table 1.

## A. Deployment and Inflation

Deployment of the parachute (i.e., mortar firing) is intended to occur at a specified dynamic pressure. Using data from on-board accelerometers, and assumptions about the entry vehicle's drag area, the flight computer calculates the time at which the mortar should fire to obtain the desired dynamic pressure at deployment. The

baseline deployment dynamic pressure for both MER A and B was 700 Pa. However, dust storms on Mars in the weeks prior to entry forced an increase in the deployment dynamic pressure for both entry vehicles in order to maintain the desired time from parachute deployment to Rocket Assisted Descent (RAD) initiation. As shown in Table 1, the deployment dynamic pressure target for MER A became 725 Pa.<sup>6</sup> Following examination of the entry data from MER A, the operations team decided to increase the MER B target deployment dynamic pressure even further to 750 Pa.<sup>6</sup> Reconstructions of the entries from accelerometer data indicate that mortar firing occurred at nominal values of 729 Pa and 765 Pa for MER A and B, respectively. The close agreement between the target and reconstructed values of dynamic pressure at deployment is an indication of the proper functioning of the mortar firing timing hardware and software. There is a  $\pm 10$  percent uncertainty in the deployment dynamic pressure as calculated by both the flight software (that determines the mortar firing time) and the reconstruction analysis. This uncertainty in the dynamic pressure has a common source, namely the uncertainty in the drag coefficient of the entry vehicle ( $\pm 10$  percent of the nominal value at the  $3\sigma$  level with a normal distribution). The uncertainty in the reconstructed dynamic pressure at deployment is  $\pm 73$  Pa for MER A and  $\pm 77$  Pa for MER B. Thus, the deployment dynamic pressure may have been as large as 802 Pa for MER A and 842 Pa for MER B (at the  $3\sigma$  level). Earlier reports<sup>4,7</sup> document the initial qualification of the MER parachute for a maximum deployment dynamic pressure at Mars of 810 Pa. However, an additional structural qualification test was conducted on June 23, 2003 that subjected the parachute to a peak opening load of 133,329 N – the equivalent of a deployment dynamic pressure at Mars of over 900 Pa. Therefore, the MER team was confident that the higher dynamic pressure at deployment encountered by MER B would not exceed the structural strength of the parachute.

The final pre-flight Monte Carlo analyses<sup>6</sup> yielded the parachute deployment time from entry as shown in Table 1. For both MER A and B the reconstructed values of the parachute deployment time were near the high end of the analyses range. These later-than-expected parachute deployments have been attributed to lower than expected atmospheric densities at high altitudes.<sup>6</sup> Pre-flight results for the deployment Mach number are also shown in Table 1.

**Table 1. Deployment, inflation, and terminal descent parameters**

	MER A "Spirit"	MER B "Opportunity"
<b>DEPLOYMENT</b>		
Dynamic Pressure (Pa) – Target <sup>1</sup>	725	750
Dynamic Pressure (Pa) – Reconstruction	729 $\pm$ 73	765 $\pm$ 77
Time from Entry (s) – Pre-Flight Analysis $3\sigma$ Range <sup>6</sup>	237.3-253.8	234.5-249.7
Time from Entry (s) – Reconstruction	251	250
Mach number – Pre-Flight Analysis $3\sigma$ Range <sup>6</sup>	1.71-1.85	1.78-1.94
<b>INFLATION</b>		
Time from Mortar Firing to Peak Load (s) – Pre-Flight Assumption	1.17-1.43 <sup>A</sup>	
Time from Mortar Firing to Peak Load (s) – Reconstruction	1.38-1.75 <sup>B</sup>	1.50-1.89 <sup>B</sup>
Peak Opening Load (N) – Analysis	60,190	64,406
Peak Opening Load (N) – Reconstruction	52,073	58,745
Peak Opening Load Difference – Analysis vs Reconstruction	+15.6%	+9.6%
<b>TERMINAL DESCENT</b>		
Velocity at RAD Initiation (m/s) – Pre-Flight Analysis $3\sigma$ Range <sup>6</sup>	61.6-84.5	61.4-84.1
Velocity at RAD Initiation (m/s) – Reconstruction	67.4	71.2
Parachute $C_D$ at RAD Initiation – Pre-Flight Assumption	0.384-0.488 <sup>A</sup>	
Parachute $C_D$ at RAD Initiation – Reconstruction	0.52	0.43

A) Uniform distribution between limits. B) Possible range given the accelerometer data rate.

Parachute inflation was reconstructed from the entry vehicle accelerometer data. These data were available at a rate of only 8 Hz, thus limiting the extent to which the inflation could be accurately reconstructed. In Figure 1, the reconstructed parachute opening load is plotted versus the earliest possible time at which the mortar may have fired. Mortar recoil is clearly shown by the negative loads, although the peak mortar recoil load is not captured by the 8 Hz data. Inflation begins once the parachute is out of its deployment bag and can be identified by the rapid increase in parachute opening load. Although the rate at which the inflations proceeded once they started are approximately the same for both MER A and B, inflation on MER B started about 0.15 seconds later. Again, the 8

Hz data rate limits the ability to determine exactly when the peak opening loads occurred – the actual peaks almost certainly occurred at times between the available data points.

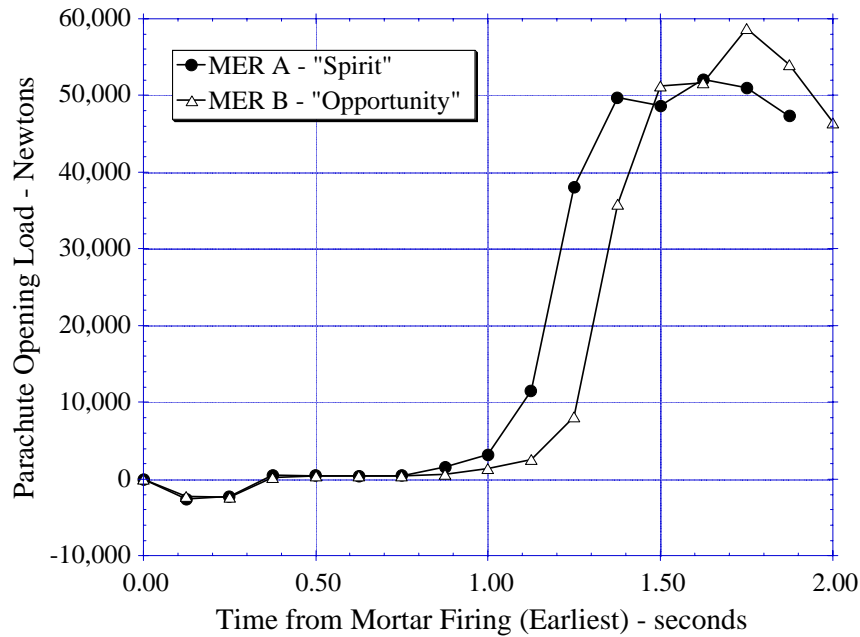


**Figure 1. Parachute opening load reconstruction.**

As shown in Table 1, the pre-flight assumption for the time from mortar firing to peak load was between 1.17 and 1.43 seconds. The reconstruction for MER A placed it between 1.38 and 1.75 seconds. Thus for MER A these time intervals overlap. The same is not true of MER B where the reconstructed time from mortar firing to peak load is 1.50 to 1.89 seconds. Nevertheless, the data indicate that deployment and inflation for both MER A and B proceeded without anomalies.

The reconstructed peak opening loads for MER A and B are 52,073 and 58,745 N, respectively. These values almost certainly underestimate the peak load since inflation is a short duration event that was probably missed by the low sampling rate from the accelerometer. Analyses for the corresponding reconstructed nominal values of the dynamic pressure at deployment (i.e., 729 and 765 Pa for MER A and B, respectively) yield peak opening loads of 60,190 N for MER A and 64,406 N for MER B. These values are higher than the reconstructed values for the reason already noted, but are probably more accurate estimates of the actual peak opening loads.

## B. Terminal Descent

The terminal descent performance of the parachutes was evaluated using the radar data and atmospheric models. For MER A the pre-flight analyses<sup>6</sup> yielded a  $3\sigma$  velocity range at RAD initiation of 61.6 to 84.5 m/s as shown in Table 1. The reconstructed radar velocity at RAD firing is 67.4 m/s, well within the expected range. Similarly, for MER B, the reconstructed radar velocity at RAD initiation is 71.2 m/s; again, well within the pre-flight analyses  $3\sigma$  range of 61.4 to 84.1 m/s.

The nominal value of the MER parachute drag coefficient,  $C_D$ , at subsonic speeds was determined from wind tunnel tests<sup>8</sup> and found to be 0.436. For Monte Carlo simulations the parachute  $C_D$  at subsonic speeds was assumed to have a range from 0.384 to 0.488 with a uniform distribution between these limits. To obtain the reconstructed drag coefficient of the parachute at RAD initiation, the radar data and final pre-flight atmospheric models were used. The reconstructed values of  $C_D$  at RAD initiation for MER A and B are 0.52 and 0.43, respectively. For MER A this value of  $C_D$  falls outside the assumed range, whereas for MER B it is near the middle of the range. However, care should be exercised in interpreting these results since the reconstructed drag coefficient values have large uncertainties due primarily to the atmospheric model. The atmospheric density required for the calculation of  $C_D$  comes from a model of the Martian atmosphere, not from in-situ measurements. There is also no instrumentation on the rovers that allows for direct calculation of the atmospheric density at the surface.

No numerical comparisons were performed between pre-flight analyses and flight data with regards to stability during the parachute phase. However, reconstructed animations of the parachute phase (using IMU data sampled at 8 Hz) for both landings using the flight data showed motions similar to those seen in the pre-flight analyses animations.

### **III. Conclusion**

The Mars Exploration Rover mission successfully landed two rovers on the surface of Mars in 2004. Key to this was the performance of the parachute system during Entry, Descent, and Landing. The models for Disk Gap Band parachute performance were further validated by the returned flight data. Unfortunately, the returned data was of insufficient detail to perform detailed analysis and characterization of critical performance parameters. In addition, the lack of atmospheric data following landing prevents detailed understanding of canopy drag performance.

Current numerical models for this canopy type were validated to the variation ranges assumed. The drag coefficient for this type DGB is within the range of 0.38 to 0.52, including all sources. The deployments occurred at dynamic pressures between 730 and 764 Pa at a Mach number from 1.71 to 1.94. However, uncertainty in atmospheric properties suggest that the dynamic pressure could have been as high as 842 Pa or as low as 656 Pa. Peak inflation loads were difficult to assess from returned data and are assumed to be well within the limits suggested by pre-landing analyses (64.5 kN).

### **Acknowledgments**

This work was performed in association with the Jet Propulsion Laboratory, California Institute of Technology, under a contract with the National Aeronautics and Space Administration.

### **References**

1. Witkowski, A. and Bruno, R.: Mars Exploration Rover Parachute Decelerator System Program Overview, AIAA Paper 2003-2100, 2003.
2. Vasas, R. and Styner, J.: Mars Exploration Rover Parachute Mortar Deployer Development, AIAA Paper 2003-2137, 2003.
3. McEwan, A. J.: An Investigation of Parachute Opening Loads, and a New Engineering Method for their Determination, AIAA Paper 70-1168, 1970.
4. Cruz, J. R., Kandis, M., and Witkowski, A.: Opening Loads Analyses for Various Disk-Gap-Band Parachutes, AIAA Paper 2003-2131, 2003.
5. Barnard, G. A.: The Effect of Extreme Altitude on Parachute Filling Distance, AIAA Paper 93-1207, 1993.
6. Desai, P. N. and Knocke, P. C.: Mars Exploration Rovers Entry, Descent, and Landing Trajectory Analysis, AIAA Paper 2004-5092, 2004.
7. Zell, P. T., Cruz, J. R., and Witkowski, A.: Structural Testing of Parachutes in the National Full-Scale Aerodynamics Complex 80-by-120-Foot Wind Tunnel at NASA Ames Research Center, AIAA Paper 2003-2130, 2003.
8. Cruz, J. R., Mineck, R. E., Keller, D. F., and Bobskill, M. V.: Wind Tunnel Testing of Various Disk-Gap-Band Parachutes, AIAA Paper 2003-2129, 2003.